Short Range Structure of Amorphous $Ni_{50}Ta_{50}$-Alloys by Means of X-Ray- and Neutron-Diffraction

H. Uhlig, L. Rohr*, H.-J. Güntherodt*, P. Fischer**, P. Lamparter, S. Steeb

Max-Planck-Institut für Metallforschung, Institut fürWerkstoffwissenschaft, Stuttgart, Germany

Z. Naturforsch. **47a**, 826–832 (1992); received May 7, 1992

Dedicated to Prof. Dr. H. F. Fischmeister in occasion of his 65th birthday

Amorphous $Ni_{50}Ta_{50}$-samples with their high crystallization temperature of 985 K were investigated. To evaluate the three partial structure factors of amorphous $Ni_{50}Ta_{50}$ one X-ray diffraction experiment was performed with $Ni_{50}Ta_{50}$ and two neutron diffraction experiments with $Co_{10}Ni_{40}Ta_{50}$ and with $Ni_{50}Ta_{50}$, respectively. The Bhatia-Thornton partial structure factor $S_{CC}(Q)$ indicates rather strong chemical short range order which also explains the premaximum observed in the Faber-Ziman partial $S_{NiNi}(Q)$-function. The nearest neighbor distance is 2.82 Å for Ni–Ni, 2.91 Å for Ta–Ta, and is shortest for Ni–Ta, 2.44 Å. The coordination numbers are $N_{NiNi}=4.9$, $N_{TaTa}=8.2$, and $N_{NiTa}=6.0$.

We report on the chemical short range order and the possible binding behavior in a-$Ni_{50}Ta_{50}$ and compare the present results with those reported in the literature on a-$Ni_{40}Ti_{60}$ as well as on a-$Ni_{55}Ta_{45}$.

1. Introduction

Amorphous Ni_xTa_{1-x}-alloys ($0.3 \leq x \leq 0.68$) were prepared using the splat cooling method with levitation melting in vacuum [1]. These alloys show rather high crystallization temperatures between 1030 K and 950 K [1]. The Vickers hardness amounts to the rather high value of about 900 kp/mm^2. The resistivity and Hall effect was measured also [2]. Possible applications of these alloys are as substrates for chips and as films for brazing [2].

In the present paper we report on the determination of partial structure factors by combination of X-ray- and neutron-diffraction with the amorphous $Ni_{50}Ta_{50}$-alloys (crystallization temperature 985 K; melting point of the corresponding crystalline alloy 1930 K). Three diffraction experiments are necessary, which have to differ in the scattering length of at least one of the components. We will show that this can be achieved in the present case of amorphous $Ni_{50}Ta_{50}$ first in proving by the investigation of an amorphous (a)-$Co_{50}Ta_{50}$-alloy that Ni can be isomorphously substituted by Co. Secondly neutron diffraction was applied not only to a-$Ni_{50}Ta_{50}$ but also to a-$Co_{10}Ni_{40}Ta_{50}$, and thirdly an X-ray diffraction experiment was performed with a-$Ni_{50}Ta_{50}$.

As usual, the partial structure factors will yield the pair correlation functions, atomic distances, partial coordination numbers as well as hints on the binding behaviour.

* Institut für Physik, Universität Basel, CH-4056 Basel, Switzerland.

** Labor für Neutronenstreuung, ETHZ, CH-5232 Villigen PSI, Switzerland.

Reprint requests to Prof. Dr. S. Steeb, Max-Planck-Institut für Metallforschung, Institut für Werkstoffwissenschaft, Seestraße 92, W-7000 Stuttgart 1.

2. Theoretical Fundamentals

From the coherently scattered intensity $I_{coh}(Q)$ one obtains the total structure factor $S^{FZ}(Q)$ according to Faber and Ziman [3]:

$$S^{FZ}(Q) = \frac{I_{coh}(Q) - c_1 c_2 (b_1 - b_2)^2}{\langle b \rangle^2} \qquad (1)$$

with

$Q = 4\pi (\sin \Theta)/\lambda$ = modulus of the momentum transfer,

2Θ = diffraction angle,

λ = wavelength of the scattered radiation,

c_i = concentration of component i in atomic fractions,

b_i = scattering length of component i for coherent scattering,

$\langle b \rangle = c_1 b_1 + c_2 b_2$.

$S^{FZ}(Q)$ is the weighted sum of the partial structure factors $S_{ij}^{FZ}(Q)$, which describes the contribution of

0932-0784 / 92 / 0700-0826 $ 01.30/0. – Please order a reprint rather than making your own copy.

ij-pairs to the structure factor:

$$S^{FZ}(Q) = \frac{c_1^2 b_1^2}{\langle b\rangle^2} S_{11}(Q) + \frac{2c_1 c_2 b_1 b_2}{\langle b\rangle^2} S_{12}(Q) + \frac{c_2^2 b_2^2}{\langle b\rangle^2} S_{22}(Q). \quad (2)$$

This equation shows that each partial structure factor is multiplied by a weighting factor W_{ij} which contains the concentrations and the scattering lengths.

By Fourier-transformation follows the total reduced pair distribution function $G^{FZ}(R)$ in real space which is composed of the partial functions $G_{ij}(R)$ using the same weighting factors as in (2).

For the understanding of structural results it is useful to adopt also the description according to Bhatia and Thornton [4]. For the total Bhatia-Thornton structure factor stands:

$$S^{BT}(Q) = \frac{I_{coh}(Q)}{\langle b^2\rangle} = \frac{\langle b\rangle^2}{\langle b^2\rangle} S_{NN}(Q) + \frac{c_1 c_2 (b_1 - b_2)^2}{\langle b^2\rangle} S_{CC}(Q) + 2\frac{\langle b\rangle (b_1 - b_2)}{\langle b^2\rangle} S_{NC}(Q) \quad (3)$$

with

$S_{NN}(Q)$ = contribution of density-density correlations,
$S_{CC}(Q)$ = contribution of concentration-concentration correlations,
$S_{NC}(Q)$ = contribution of concentration-density correlations.

The Fourier transform of $S^{BT}(Q)$ yields the BT total reduced pair distribution function $G^{BT}(R)$, which is composed of the partial BT pair distribution functions $G_{NN}(R)$, $G_{CC}(R)$, and $G_{NC}(R)$ using the same weighting factors as in (3).

The connection between both formalisms is given for example by

$$G_{CC}(R) = c_1 c_2 [G_{11}(R) + G_{22}(R) - 2G_{12}(R)]. \quad (4)$$

3. Experimental

3.1. Specimen Preparation

From Ta (purity 99.9%), Ni (purity 99.98%), and Co (purity 99.99%) alloy buttons were made by melting the constituents together in argon atmosphere. The buttons were turned over and remelted several times in order to ensure homogeneity. The alloys were broken into 400 mg sections and rapidly quenched from the melt within a two piston splat-cooling device. The resulting splats were 40–60 μm thick and 15–25 mm wide.

3.2. How to Obtain Partial Structure Factors from the Total Structure Factors

For the evaluation of the partial Faber-Ziman structure factors according to (2) one needs three experimental total structure factors with different weighting factors, i.e. three independent equations which present a linear independent 3×3 system. In the present work we applied the combination of two neutron- with one X-ray-diffraction experiment. In the following we discuss the Q-dependence of the Faber-Ziman weighting factors, which is shown in Figure 1 a. Whereas the weighting factors W_{NiNi} and W_{NiTa} decrease, the weighting factor W_{TaTa} increases with increasing Q. The sum of $\sum_j W_{ij}$ must be one. We used the complex X-ray scattering amplitudes $b(Q) = b_0(Q) + b' + ib''$. $b_0(Q)$ was taken from [5], b' and b'' from [6].

The calculation of the three weighting factors for a neutron experiment with a-$Co_{50}Ta_{50}$ using the

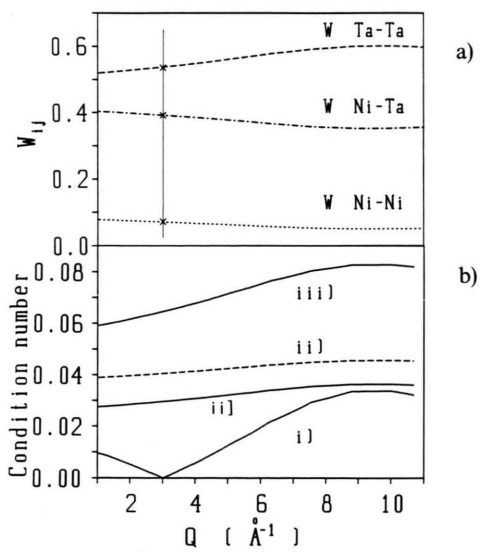

Fig. 1 a. Faber-Ziman X-ray weighting factors for the $Ni_{50}Ta_{50}$-alloy. The neutron weighting factors for a-$Co_{50}Ta_{50}$ are marked with (×).
Fig. 1 b. Q-dependence of the condition number; (——) Faber-Ziman formalism; (– – –) Bhatia-Thornton formalism.
i) n $Ni_{50}Ta_{50}$; n $Co_{50}Ta_{50}$; x $Ni_{50}Ta_{50}$,
ii) n $Ni_{50}Ta_{50}$; n $Co_{10}Ni_{40}Ta_{50}$; x $Ni_{50}Ta_{50}$,
iii) n $Ni_{50}Ta_{50}$; n $Co_{25}Ni_{25}Ta_{50}$; x $Ni_{50}Ta_{50}$.

neutron scattering lengths according to [7] yields that these coincide with the X-ray weighting factors at $Q = 3$ Å^{-1}. The corresponding values are marked by crosses ($\times$) in Figure 1 a.

Figure 1 b shows the Q-dependence of the condition number, i.e. the normalized determinant of the weighting factors for the following three combinations of experiments:

i) n $Ni_{50}Ta_{50}$; n $Co_{50}Ta_{50}$; x $Ni_{50}Ta_{50}$;
ii) n $Ni_{50}Ta_{50}$; n $Co_{10}Ni_{40}Ta_{50}$; x $Ni_{50}Ta_{50}$;
iii) n $Ni_{50}Ta_{50}$; n $Co_{25}Ni_{25}Ta_{50}$; x $Ni_{50}Ta_{50}$.

The combination i) shows the lowest value and reaches zero for $Q = 3$ Å^{-1}, which means that for this Q-surrounding the system is too ill-conditioned. The combination iii) shows the highest value and thus would be most convenient for the solution of the present problem.

However, to be sure that the method of isomorphous substitution is not disturbed by the slight difference of atomic volumes of nickel and cobalt, respectively, we chose the combination ii). The full-line curves in Fig. 1 b are calculated for the Faber-Ziman formalism. The condition number as calculated for the Bhatia-Thornton formalism and combination ii) is shown as dashed line.

3.3. Diffraction Methods

3.3.1. X-ray Diffraction

X-ray diffraction with a-$Ni_{50}Ta_{50}$ was done in reflection mode using Ag-Kα-radiation with graphite monochromator in the diffracted beam.

The experimentally obtained intensity curve was corrected for polarization [8], Compton scattering [5, 8], and then normalized to $S(Q)$ [9].

3.3.2. Neutron Diffraction

Neutron diffraction with the a-$Ni_{50}Ta_{50}$-specimen (10 grams) was performed with the powder diffractometer DMC [10] using $\lambda = 1.0862$ Å at the research reactor Saphir of Paul Scherrer Institute (Villigen, Switzerland). The scattered radiation was detected by a multidetector covering a 2Θ-range of 80° which was placed at two measuring positions with an overlap of about 26°. Thus the total 2Θ-range was 134°.

Neutron diffraction with the a-$Co_{10}Ni_{40}Ta_{50}$-specimen (4.23 grams) was done with the two axes diffractometer 7 C 2 using $\lambda = 0.699$ Å at the hot source of the research reactor Orphée (Saclay, France). The detection also was done using a multidetector covering a 2Θ-range of 128°.

The experimentally obtained intensity curves were corrected for absorption [11], multiple scattering [12], inelastic scattering [13], and then normalized to $S(Q)$ [9].

3.3.3. Combination of X-ray- and Neutron Data

To eliminate the influence of rounding errors during the calculation of the partial structure factors it proved to be commendable to apply the method of iterative refinement [14]. For the explanation of this method we start with the equation

$$\boldsymbol{S}_{\text{tot}}(Q) = A(Q) \cdot \boldsymbol{S}_{\text{part}}(Q) \tag{5}$$

with

$\boldsymbol{S}_{\text{tot}}(Q)$ = vector presentation of the total structure factors.
$A(Q)$ = matrix containing the weighting factors from (2), (3). The matrix becomes Q-dependent since the scattering lengths for X-rays are Q-dependent.
$\boldsymbol{S}_{\text{part}}(Q)$ = vector presentation of the partial structure factors.

Inversion of (5) yields

$$\boldsymbol{S}_{\text{part}}(Q) = A^{-1}(Q)\, \boldsymbol{S}_{\text{tot}}(Q)\,. \tag{6}$$

In the ideal case

$$\boldsymbol{S}_{\text{tot}}(Q) - A(Q) \cdot \boldsymbol{S}_{\text{part}} = 0 \tag{7}$$

should hold. In reality, however, a residual $\boldsymbol{R}(Q)$ due to rounding errors for the total structure factor remains instead of zero:

$$\boldsymbol{S}_{\text{tot}}(Q) - A(Q) \cdot \boldsymbol{S}_{(i-1)\,\text{part}} = \boldsymbol{R}_i(Q)\,. \tag{8}$$

According to (6) the residual $\boldsymbol{P}_i(Q)$ for the partial structure factors follows as

$$\boldsymbol{P}_i(Q) = A^{-1}(Q) \cdot \boldsymbol{R}_i(Q)\,. \tag{9}$$

Following (10), the partial structure factors are refined by the recursion

$$\boldsymbol{S}_{i\,\text{part}} = \boldsymbol{S}_{(i-1)\,\text{part}} + \boldsymbol{P}_i\,. \tag{10}$$

4. Results and Discussion

4.1. Reciprocal Space

Figure 2 shows the total structure factors for a-$Ni_{50}Ta_{50}$ as obtained with X-rays (lower curve) as well as with neutrons. The curves are rather similar with a pronounced first maximum and a splitted up second maximum, which is followed by a third and fourth maximum. The maxima in the middle curve, especially also in the upper curve are shifted to higher Q-values compared with the lower curve. This can be explained by the fact that with neutrons the element Ni with its smaller atomic diameter has the larger scattering length, whereas with X-rays Ta is the stronger scatterer.

Figure 3 shows the three partial Faber-Ziman structure factors as obtained from Fig. 2 using the method of iterative refinement (see Chapter 3.3.3).

The Ta–Ta-curve shows the lowest noise, followed by the Ni–Ta curve and, with the largest noise, the Ni–Ni curve. With all three curves the main peak is followed by a double peak (second maximum) as well as a third and fourth maximum. At about 1.6 $Å^{-1}$ we observe in the Ni–Ni curve a prepeak which indicates compound formation.

In Figure 4 we present the partial Bhatia-Thornton structure factors for a-$Ni_{50}Ta_{50}$. They were calculated from the experimental $S^{BT}(Q)$ via (3) using the method of iterative refinement. The $S_{NN}(Q)$-curve is caused by the topological arrangement of the atoms independent from the atomic species. The $S_{CC}(Q)$-curve is determined by the distribution of the atoms of different kinds within the amorphous $Ni_{50}Ta_{50}$-specimen. Its pronounced oscillations are a hint on strong chemical ordering effects. This follows also from the prepeak at 1.6 $Å^{-1}$ which occurred in $S_{NiNi}(Q)$ (see Figure 3).

Oscillations in the S_{NC}-curve are caused by differences of the atomic volumes of both components. This curve shows the usual behaviour.

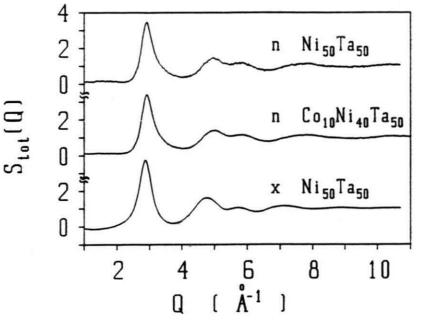

Fig. 2. Amorphous $Ni_{50}Ta_{50}$ and amorphous $Co_{10}Ni_{40}Ta_{50}$; total Faber-Ziman structure factors; X-rays (x) and neutrons (n).

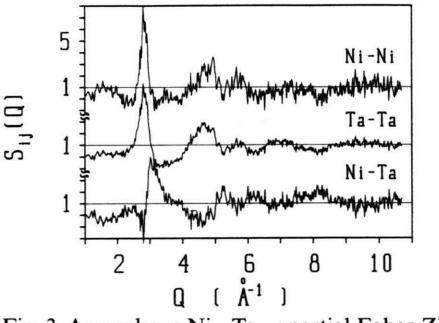

Fig. 3. Amorphous $Ni_{50}Ta_{50}$; partial Faber-Ziman structure factors.

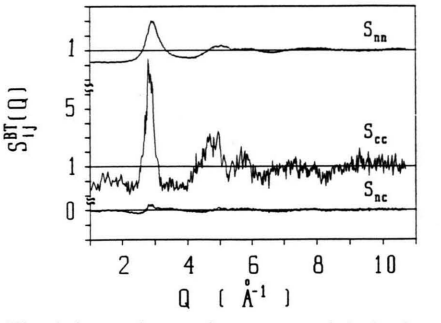

Fig. 4. Amorphous $Ni_{50}Ta_{50}$; partial Bhatia-Thornton structure factors.

4.2. Real Space

4.2.1. Faber-Ziman Pair Correlation Functions

4.2.1.1. Atomic Distances and Partial Coordination Numbers

Figure 5 shows the Faber-Ziman partial pair correlation functions which follow from the partial structure factors in Figure 3. The $G_{NiNi}(R)$- and $G_{TaTa}(R)$-curves are very similar. The maxima below 2 Å and at 3.5 Å could be identified as caused by the truncation effect, i.e. they are not physically relevant. The $G_{NiTa}(R)$-curve is also similar to the $G_{NiNi}(R)$- and $G_{TaTa}(R)$-curve.

Table 1 shows the atomic distances and partial coordination numbers. During the calculation of the

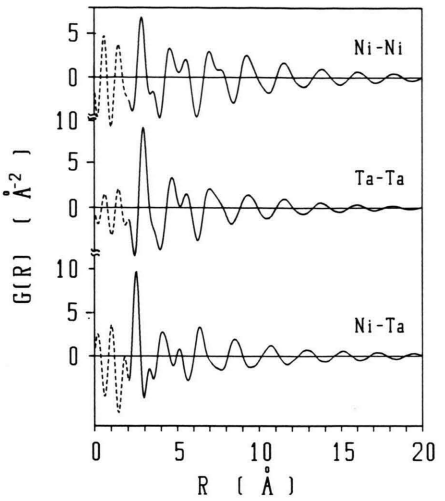

Fig. 5. Amorphous $Ni_{50}Ta_{50}$; partial Faber-Ziman pair correlation functions.

Table 1. Amorphous $Ni_{50}Ta_{50}$; atomic distances and partial coordination numbers as well as atomic diameters D_{atomic} [15].

$i-j$	R_{ij} [Å]	N_{ij}	D_{atomic} [Å]
Ni–Ni	2.82	4.9	2.48
Ta–Ta	2.91	8.2	2.98
Ni–Ta	2.44	6.0	2.73
Ta–Ni	2.44	6.0	2.73

Table 2. R/R_{ij} from G_{ij} of a-$Ni_{50}Ta_{50}$ (this paper); a-$Ni_{40}Ti_{60}$ [18]; model [17].

G_{NiTa}	1.00	1.66	2.05	2.58	2.97	3.50	
G_{TaTa}	1.00	1.60	1.93	2.40	3.11	3.31	
G_{NiNi}	1.00	1.64	2.00	2.46	2.91	3.26	3.49
model	1.00	1.65	1.99	2.49	2.97	3.38	
G_{NiTi}	1.00	1.74	1.91	2.61	2.92	3.57	
G_{TiTi}	1.00	1.56	1.81	2.39	2.74	3.20	
G_{NiNi}	1.00	1.64	1.94	2.63	2.97	3.45	

N_{ij} the hump at 3.48 Å mentioned above was disregarded.

For the density of a-$Ni_{50}Ta_{50}$ the calculated value 13.75 g cm^{-3} was used. The total number of atoms surrounding one Ni-atom amounts to 10.9 and for Ta as center-atom to 14.2.

The experimental Ni–Ta distance of 2.44 Å is smaller than the sum of the atomic radii of Ni and Ta, which means strong Ni–Ta-binding. The experimental Ta–Ta distance of 2.91 Å corresponds well to the metallic bound Ta–Ta-distance of 2.98 Å. The experiment shows furthermore that the Ni–Ni-distance is enlarged up to 2.82 Å, i.e. the Ni-atoms do not occur in close contact.

4.2.1.2. Structural Unit

In order to develop a structural unit for amorphous $Ni_{50}Ta_{50}$ the following facts must be taken into consideration: First, the premaximum in S_{NiNi} demands a Ni–Ni-distance which is enlarged by insertion of Ta-atoms. Second, the shortest experimental distances between Ni–Ta and Ta–Ta must occur in the structural unit.

In the present case an octahedron with four Ta-atoms at the four corners of the square which is capped by two Ni-atoms corresponds well with the measured distances. If the distance between the Ta–Ta pairs is designed with a, the distance between the Ni-pair with $2b$, and the Ni–Ta distance with x, then

$$x = \sqrt{\frac{a^2}{2} + b^2}\,. \tag{11}$$

Using the distances $a = 2.91$ Å and $b = 1.41$ Å from Table 1 we obtain from (11) the calculated value $x_{calc} = 2.49$, which corresponds well to the experimental value $x = 2.44$ Å.

In [16] we will present an improved structural unit for the present case of a-$Ni_{50}Ta_{50}$.

On the other hand, in Table 2 we have compiled in the upper part for a-$Ni_{50}Ta_{50}$ the positions of the maxima in $G_{ij}(R)$ after normalization to the position R_{ij} of the first maximum. The table also contains the normalized positions as obtained in [17] for a tetrahedral close packing model. The comparison shows that this model describes the maxima positions of all three partial functions rather well.

4.2.2. Bhatia-Thornton Partial Pair Correlation Functions

Figure 6 shows the Bhatia-Thornton partial functions $G_{NN}(R)$, $G_{CC}(R)$, and $G_{NC}(R)$. $G_{NN}(R)$ shows a so called normal run with a pronounced main peak, which is followed by a split up second peak, etc.

The oscillations of $G_{CC}(R)$ point to a distinct chemical ordering effect.

According to (4) maxima in $G_{CC}(R)$ mean $G_{11} + G_{22} > 2G_{12}$ and minima in $G_{CC}(R)$ mean $2G_{12} > G_{11} + G_{22}$. Starting at $R = 2$ Å, in the smallest coordina-

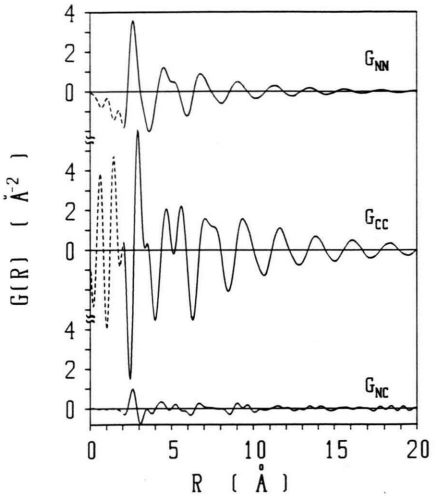

Fig. 6. Amorphous $Ni_{50}Ta_{50}$; partial Bhatia-Thornton pair correlation functions.

Table 3. Amorphous $Ni_{50}Ta_{50}$. Bhatia-Thornton partial functions. Positions of maxima and minima.

$G_{NN}(R)$	R_{max} [Å]	2.57	4.50	5.15	6.75	9.0	
$G_{CC}(R)$	R_{max} [Å]		2.89	4.63	5.56	7.08	7.59
	R_{min} [Å]	2.44	3.99		6.30		8.44
$G_{NC}(R)$	R_{max} [Å]	2.57	4.50	5.21	6.69	9.0	

i–j	R_{ij} [Å]	N_{ij}
Ni–Ni	2.63	2.27
Ti–Ti	3.01	8.05
Ni–Ti	2.60	7.91

Table 4. Amorphous $Ni_{40}Ti_{60}$; atomic distances and partial coordination numbers [18].

i–j	R_{ij} [Å]	N_{ij}
Ni–Ni	2.52	5.3
Ta–Ta	3.06	6.4
Ni–Ta	2.78	6.2
Ta–Ni	2.78	7.6

Table 5. Amorphous $Ni_{55}Ta_{45}$; atomic distances and partial coordination numbers [19].

tion sphere the unlike pairs are dominant whereas in the second sphere with radius $R = 2.89$ Å the pairs of equal atoms prevail.

The $G_{NC}(R)$-function is determined by the difference between the atomic volumes and shows the usual behaviour.

Table 3 contains the positions of the maxima in $G_{NN}(R)$ as well as $G_{NC}(R)$ and of the maxima and minima in $G_{CC}(R)$.

4.2.3. Amorphous $Ni_{50}Ta_{50}$ and Amorphous $Ni_{40}Ti_{60}$

The elements Ti and Ta are chemically rather similar. The difference of the electronegativities amounts to 0.1 for Ni–Ti and 0.1 for Ni–Ta. The covalent radius amounts to 1.32 Å for Ti and 1.34 Å for Ta, the atomic radius to 1.47 Å for Ti and 1.49 Å for Ta. In [18] the partial pair correlation functions were evaluated for a-$Ni_{40}Ti_{60}$ using the method of isotopic substitution. Table 4 contains the atomic distances and partial coordination numbers for amorphous $Ni_{40}Ti_{60}$ [18]. The comparison with Table 1 shows that R_{NiTi} is the shortest distance in a-$Ni_{40}Ti_{60}$ as R_{NiTa} in a-$Ni_{50}Ta_{50}$.

The partial coordination number N_{NiNi} is rather small compared with 4.9 (Table 1) for a-$Ni_{50}Ta_{50}$. But the $G_{NiNi}(R)$-curve shows a very strong second maximum at $R^{II}_{NiNi} = 4.16$ Å. Using this Ni–Ni-distance together with R_{TiTi} from Table 4, we obtain, using (11), for the distance $R_{NiTi} = 2.97$ Å. This distance is too large. In the case of a-$Ni_{40}Ti_{60}$ a triangular double pyramid yields $R_{NiTi,\,calc.} = 2.71$ Å which is in good agreement with the experimental value in Table 4.

In Table 2 we find the normalized distances from G_{NiNi}, G_{TiTi}, and G_{NiTi} in comparison to the tetrahedral close packing model, and we state that also for a-$Ni_{40}Ti_{60}$ all values agree quite well.

4.2.4. Amorphous $Ni_{55}Ta_{45}$

In [19] three partial functions were evaluated from one neutron- and one X-ray diffraction experiment with meltspun a-$Ni_{55}Ta_{45}$ as well as one neutron diffraction experiment with meltspun a-$Ni_{62}Ta_{38}$. The condition number for this combination amounts to 0.06.

In Table 5 the corresponding atomic distances and partial coordination numbers are listed.

From Table 5 we learn that according to [19] for a-$Ni_{55}Ta_{45}$ not the Ni–Ta-distance but the Ni–Ni-distance is the shortest. The discrepancy between [19] and the present paper cannot be explained by the fact that in the present paper splat cooled samples were used whereas in [19] meltspun samples were under investigation. Also the different alloy compositions, namely $Ni_{55}Ta_{45}$ in [19] compared with $Ni_{50}Ta_{50}$ in the present paper cannot explain the discrepancies. Thus there is a call for precise neutron diffraction experiments with a-$Ni_{50}Ta_{50}$ using the method of iso-

topic substitution. With the results of such measurements one will be able to decide whether the method of isomorphous substitution as applied here with a condition number of 3%, or the method of concentration variation with a condition number of 6%, as applied in [19], is more reliable. At this moment we can only state that despite the very good experimental total structure factors the rather ill-conditioned systems of linear equations in the present paper or in [19], respectively, supply us with very contradictory results.

5. Conclusion

Using the splat cooling method with levitation melting in vacuum, amorphous $Ni_{50}Ta_{50}$ as well as amorphous $Co_{10}Ni_{40}Ta_{50}$ was produced. Each of the specimens was investigated by neutron diffraction and the a-$Ni_{50}Ta_{50}$ furthermore by X-ray diffraction. The system of three linear equations for the calculation of the three partial structure factors from the total structure factors has a condition number of 3%. During the evaluation of the data the method of iterative refinement was applied. The Bhatia and Thornton partial $S_{CC}(Q)$-structure factor indicates rather strong compound formation in a-$Ni_{50}Ta_{50}$. The partial Ni–Ni structure factor shows a prepeak which is a hint on chemical ordering effects. The shortest Ni–Ni distance is 2.82 Å. The distance between unequal pairs amounts to 2.44 Å and is shorter than the mentioned Ni–Ni distance or the Ta–Ta-distance of 2.91 Å. Those three distances describe rather well a square double pyramid. The normalized positions of maxima of $G_{NiNi}(R)$, $G_{TaTa}(R)$, and $G_{NiTa}(R)$ correspond to those given by the tetrahedral close packing model of Takeuchi. The better model also applies to a-$Ni_{40}Ti_{60}$. The structural unit of this alloy is a triangular double pyramid and in so far different from the square double pyramid of a-$Ni_{50}Ta_{50}$.

We discuss the present data also together with the literature data for meltspun a-$Ni_{55}Ta_{45}$ and recognize strong contradictions since with a-$Ni_{55}Ta_{45}$ not the distance between Ni–Ta-pairs (2.78 Å) is the shortest but the Ni–Ni-distance (2.52 Å). The consequence is that with a-$Ni_{50}Ta_{50}$ neutron diffraction experiments using the method of isotopic substitution should be done for final clarification.

Acknowledgement

Thanks are due R. Bellissent, LLB Saclay, for beamtime at the 7C2 instrument.

[1] T. Richmond, L. Rohr, P. Reimann, G. Leeman, and H.-L. Güntherodt, Proceedings RQ7 (1990) 63.
[2] L. Rohr, P. Reimann, T. Richmond, and H.-J. Güntherodt, Proceedings RQ7 (1990) 715.
[3] T. E. Faber and J. M. Ziman, Phil. Mag. **11**, 153 (1965).
[4] A. Bhatia and D. E. Thornton, Phys. Rev. B **2**, 3004 (1970).
[5] J. H. Hubbell et al., J. Phys. Chem. Ref. Data **4**, 2130 (1975).
[6] Y. Waseda, Novel Application of Anomalous (Resonance) X-ray Scattering for Structural Characterization of Disordered Materials, Springer-Verlag, Berlin 1984.
[7] L. Koester, H. Rauch, and E. Seymann, Atomic Data and Nuclear Data Tables **49**, 65 (1991).
[8] C. N. J. Wagner, J. Non-Cryst. Solids **31**, 1 (1978).
[9] J. Krogh-Moe, Acta Cryst. **9**, 951 (1956).
[10] J. Schefer, P. Fischer, H. Heer, A. Isacson, M. Koch, and R. Thut, Nucl. Instrum. Meth. A **288**, 477 (1990).
[11] H. H. Paalman and L. J. Pings, J. Appl. Phys. **33**, 2635 (1962).
[12] V. F. Sears, Adv. Phys. **24**, 1 (1975).
[13] G. Placzek, Phys. Rev. **31**, 377 (1952).
[14] Å. Björck and G. Dahlquist, Numerische Methoden 1972, R. Oldenbourg, München.
[15] Catalogue Number 9 – 18806, Page 2, Sargent-Welsh, Scientific Comp. 1968.
[16] S. Steeb and P. Lamparter, Proc. LAM 8, Vienna (Aug. 31–Sept. 4, 1992) 1993.
[17] S. Takeuchi and S. Kobayashi, Phys. Stat. Sol. (a) **65**, 315 (1981).
[18] T. Fukunaga, N. Watanabe, and K. Suzuki, J. Non Cryst. Solids **61, 62**, 343 (1984).
[19] H. E. Fenglai, P. P. Gardner, N. Cowlam, and H. A. Davies, J. Phys. F: Met. Phys. **17**, 545 (1987)